ARTICLES

Formation Mechanism of Anthracene Dimers and Excimers in NaY Zeolitic Nanocavities

Oh-Hoon Kwon, Hyunung Yu,† and Du-Jeon Jang*

School of Chemistry (NS60), Seoul National University, Seoul 151-742, Korea

Received: July 25, 2003

The dimer and the excimer formation mechanisms of anthracene in NaY zeolitic nanocavities have been studied by using various spectroscopic techniques of ^{129}Xe NMR, diffuse reflectance, and emission as well as time-resolved fluorescence. Two anthracene molecules adsorb concertedly into a zeolitic supercage to form a ground-state stable dimer. An excited monomer in a singly occupied supercage gives birth to an excimer if another monomer exists in a tetrahedrally connected nearest supercage. An excited monomer forms a nonluminescent ion pair with a monomer in a nearest supercage by transferring an electron within 100 ps. The dark intermediate rearranges to transform into an excimer on the time scale of 400 ps.

Introduction

Zeolites have been extensively investigated, as they play indispensable roles in many technological and economical applications.[1−3] Their ordered cages and channels are potential hosts to organic and inorganic complexes, and act as nanosized reactors in the synthesis of nanoclusters and nanowires.[4−6] Furthermore, optical properties of molecular clusters confined in zeolites have been widely explored because their electronic properties can be altered by varying the dielectric and charge properties of the nanoporous hosts.[7−9] Zeolitic nanostructures may open up new nanotechnological applications for the heterogeneous catalysts and advanced electronic, magnetic, and optical devices.[10,11] There has been a great deal of research on the charaterization of organic molecules incorporated within the well-organized cavities and channels of zeolites since the interactions of zeolites with encapsulated chemical species are drastically different from the interactions of solvent molecules with solute species in a liquid phase.[12−14] In this regard, small arenes adsorbed in the supercages of faujasites have been investigated for several decades.[8,15−18] In addition to similarity to solvent shells, there are unique features that only zeolitic nanocages can provide. For example, arenes are known to have new properties in zeolitic cavities, attributed to the confinement and alignment of the molecules in the zeolitic cavities.[19−21]

Anthracene can be a good candidate for the investigations of the catalysis and heterogeneity of zeolites due to the high quantum yield and the reasonable decay time of its fluorescence.[9,22−24] Anthracene is reported[19,25,26] to form dimers in S_0 and S_1 in zeolites due to the high polarity and confinement effects of zeolitic nanocavities. Anthracene is also known to generate the cationic species in zeolitic nanocavities.[27,28]

The encapsulation of the guest molecules in the cages and channels of zeolites is also of great importance. Two methods are generally used for the encapsulation; one is diffusion by vacuum sublimation,[29] and the other is solution-phase transfer.[9] The latter method is often obscured if the size of a guest molecule approaches the pore window dimension.[12,13,30] Since the size of a molecule is similar to the pore dimension of the supercage, temperature is expected to play a crucial role in the uniform loading of anthracene in NaY. Direct experimental evidence such as $^{129}Xe-NMR$ spectra have not been shown yet on the intercalation of anthracene into faujasite zeolitic pores. $^{129}Xe-NMR$ spectroscopy has been used as a powerful tool to confirm the encapsulation of organic molecules in zeolitic nanocavities since a slight variation in the local environment of the nanocavity brings in a profound change in the chemical shift.[29,31−34]

This paper is preliminarily concerned with the successful intercalation of anthracene molecules into the supercages of NaY at the optimal temperature of 570 K prior to investigating the formation mechanisms of dimers and excimers. We have found that two anthracene molecules adsorb concertedly into a zeolitic supercage to form a ground-state stable dimer. An excited monomer in a singly occupied supercage gives birth to an excimer if another monomer exists in a tetrahedrally connected nearest supercage.

Experimental Section

Materials. Anthracene, purchased from Aldrich, was used after vacuum sublimation. NaY of high purity was synthesized, washed with doubly distilled hot water, and dried in a vacuum oven. After being dehydrated at 670 K under 10^{-5} Torr for 5 h and cooled to room temperature, NaY was found to have the typical unit cell formula of $Na_{56}(AlO_2)_{56}(SiO_2)_{136}\cdot 250H_2O$. Anthracene molecules were intercalated into zeolites by allowing anthracence vapor to diffuse into the supercage of zeolites at various temperatures under evacuated conditions. Dehydrated NaY was mixed with a known amount of anthracene in a quartz tube under N_2 atmosphere at room temperature to control the loading level of α, the molar ratio of anthracene molecules to supercages.[35] Then, the tube was evacuated, sealed, and

* Author to whom correspondence should be addressed. E-mail: djjang@plaza.snu.ac.kr.

† Present address: Department of Chemistry, University of Illinois at Urbana-Champaign, Urbana, IL 61801.

10.1021/jp0309163 CCC: $27.50
Published on Web 03/09/2004

maintained for 6 h at 570 K, if not specified otherwise, to make anthracene sublime and diffuse uniformly into zeolite supercages, and cooled slowly to room temperature. X-ray diffraction was used to confirm that the framework structure of NaY did not change during dehydration and intercalation.

Spectra. All the spectroscopic and kinetic measurements were carried out at room temperature. For ^{129}Xe−NMR study, ^{129}Xe gas (Matheson, 99.995%) was introduced into samples in NMR tubes through stopcocks at room temperature and allowed to equilibrate to 300 Torr. ^{129}Xe−NMR spectra were measured using an NMR spectrometer (Bruker, AM-300) operating at 83 MHz. The chemical shifts and the line splittings of NMR spectra were used to obtain the information on the distribution of anthracene into zeolitic nanocages. The diffuse-reflectance spectra were measured using a UV/vis scanning spectrometer equipped with an integrating sphere (Shimadzu, UV-3101 PC). Bare NaY was used for the reference material of the reflectance measurement. Emission spectra were obtained using a home-built spectrometer, which consisted of a 75-W Xe lamp (Acton Research, XS 432), two monochromators (Acton Research, Spectrapro 150 and 300 mm), and a photomultiplier tube (Acton Research, PD 438).

Fluorescence Kinetic Profiles. 320-nm pulses generated through a Raman shifter, which was filled with methane (20 atm) and pumped by the fourth harmonic pulses (266 nm) having a duration of 25 ps from a mode-locked Nd:YAG laser (Quantel, YG 701), were employed to excite samples. Fluorescence was wavelength-selected using combined band-pass filters and detected by using a CCD (Princeton Instruments, RTE−128-H) attached to a streak camera having the temporal resolution of 10 ps (Hamamatsu, C2830). Kinetic constants were extracted by fitting measured kinetic profiles to computer-simulated kinetic curves convoluted with temporal response functions iteratively.

Results and Discussion

^{129}Xe−NMR Spectra. The intercalation of anthracene molecules having dimensions of 0.9×0.5 nm^2 inside NaY supercages having 0.74-nm entrances[35] was confirmed by using ^{129}Xe−NMR spectroscopy. Intercalation temperature was varied to find out that the optimum temperature is about 570 K (Figure 1a). NaY introduced with anthracene (An−NaY) at 370 K shows a single NMR line at 83 ppm. The shift is close to the value of 78 ppm found for bare NaY,[29] indicating that anthracene molecules diffuse barely into the cavities at this condition. An−NaY prepared at 420 K shows an additional broad band at 110 ppm arising from interactions of xenon atoms with the supercages containing anthracene molecules. The large shift results from strong interactions with guest anthracene molecules adsorbed within supercages in addition to interactions with the supercage wall and other xenon atoms present in bare NaY. A single Lorentzian NMR line is known to reflect the average environment of numerous collisions of xenon atoms on the sweeping time scale of NMR, although the shift of the line is weighted by collision probabilities.[32,33] The broadness suggests that an axial gradient exists in the concentration of anthracene in the zeolitic bed of the sample.[29] The spectrum of An−NaY prepared at 520 K shows that anthracene distribution is macroscopically heterogeneous. Two lines of 107 and 126 ppm indicate that there are two different types of regions in the concentration of anthracene. However, An−NaY prepared at 570 K shows a single Lorentzian line at 116 ppm, indicating that guest molecules are homogeneously dispersed throughout the macroscopic sample volume. Of note is that the chemical shift is close to the weight-averaged value of the previous two lines. All the data hereafter were collected from samples treated at the optimum temperature of 570 K.

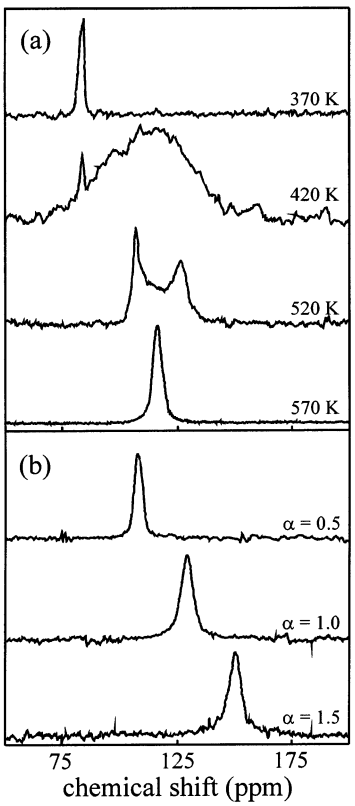

Figure 1. ^{129}Xe−NMR spectra of anthracene-introduced NaY samples as functions of the loading temperature at $\alpha = 0.5$ (a) and the loading level at 570 K (b). The chemical shifts observed at 570 K are 107 ($\alpha = 0.5$), 116 ($\alpha = 0.7$), 128 ($\alpha = 1.0$), and 151 ppm ($\alpha = 1.5$).

Figure 1b shows that the chemical shift of An−NaY increases progressively with the growth of α. The fact that the chemical shift of 151 ppm with $\alpha = 1.5$ is significantly larger than that of 128 ppm with $\alpha = 1.0$ indicates that more than one anthracene molecules can enter a single supercage to adsorb. We could not obtain proper ^{129}Xe−NMR spectra with $\alpha \geq 2$ because they were too noisy and featureless. We consider from this that the maximum number of anthracene molecules to adsorb in a supercage is two.

We are reporting ^{129}Xe−NMR spectra for the first time to our knowledge to confirm the intercalation of anthracene molecules into faujasite zeolitic nanocavities. Our ^{129}Xe−NMR spectra, sensitive probes of macroscopic distributions of molecules in zeolites, demonstrate that anthracene molecules in all the samples employed for optical measurements are successfully intercalated in the nanocavities of supercages and are homogeneously distributed throughout zeolite beds without forming clusters outside.

Diffuse-Reflectance Spectra. The diffuse-reflectance spectrum of Figure 2 with $\alpha = 0.01$ resembles the characteristic absorption spectra of anthracene solutions in vibronic structure. The spectrum results unequivocally from the π,π^* transition of the anthracene monomer, indicating that most anthracene molecules exist as monomers at this low loading level. Furthermore, the spectrum is shifted bathochromically from absorption spectra of anthracene in organic solvents, indicating that most molecules are adsorbed at very polar sites. The supercages of dehydrated faujasite zeolites are reported to be superpolar.[36] However, the vibronic bands are much less

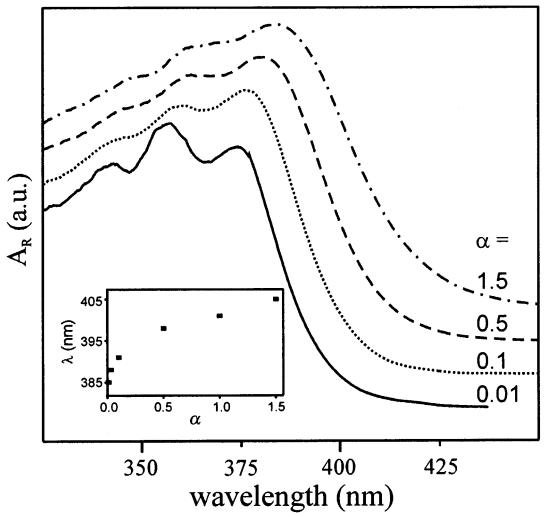

Figure 2. Diffuse-reflectance spectra of anthracene adsorbed in NaY nanocavities with indicated α values. The absorbance (A_R) was calculated by $(1 - I_R^2)/(2I_R)$, where I_R is diffuse reflectance. The inset shows the wavelength variation of the half absorbance rise from the red with α increase.

distinctive than in absorption spectra of anthracene solutions.[37] We consider that the diffused structure arises from the diverse surroundings of guest molecules intercalated in zeolitic nanocavities.

With the gradual increase of the loading level, the diffuse-reflectance spectrum shifts to the red and loses the structure of vibronic bands (Figure 2). We attribute these spectral changes to the formation of ground-state stable anthracene dimers. The inset shows that dimeric absorption increases sigmoidally with the loading level of anthracene. This suggests that dimer formation takes place concertedly. Cooperative dimer formation implies that a preoccupying anthracene molecule in a supercage exerts attractive forces on another molecule diffusing through supercages connected tetrahedrally via windows. We consider that the attractive forces favor guest molecules energetically to form dimers during cooling after the diffusion process of the sample preparation.

Fluorescence Spectra. The emission spectra of An−NaY samples show a blue band at 400 nm of monomeric fluorescence and a green band at 500 nm of excimeric one although the relative intensity of the green band increases with α increase. The blue band with $\alpha = 0.01$ shows vibronic structures more distinctively than the reflectance spectrum with $\alpha = 0.01$ in Figure 2 does. The transition bands of monomeric and dimeric species are more separated spectrally in emission than in absorption, suggesting that the photoexcited dimeric species undergoes more significant configurational relaxation in the polar environment of the nanocavity than the photoexcited monomeric species. Considering this, we speculate that an excimeric molecule has a larger dipole moment than a monomeric molecule (vide infra). At high loading levels, excimeric fluorescence prevails over monomeric one. This hints that, in addition to dimer excitation, monomer excitation also contributes to excimeric fluorescence although emission intensity depends on relaxation processes as well as population. There have been controversies on the origins of excimeric species in zeolitic nanocavities.[25,38,39] Analyzing kinetic results, we will reveal not only the formation mechanism of ground-state stable dimers but also the photochemical-formation mechanism of excimers.

Fluorescence Kinetic Profiles. While monomer fluorescence was observed at 400 nm, excimer emission was monitored at

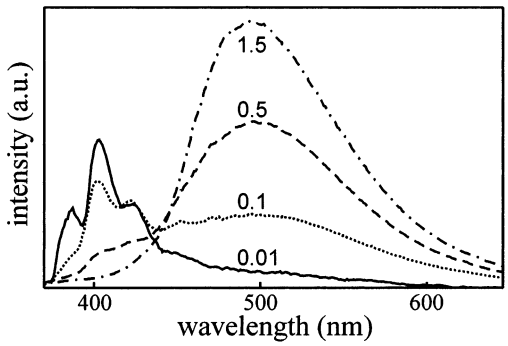

Figure 3. Emission spectra of anthracene adsorbed in NaY nanocavities with indicated α values.

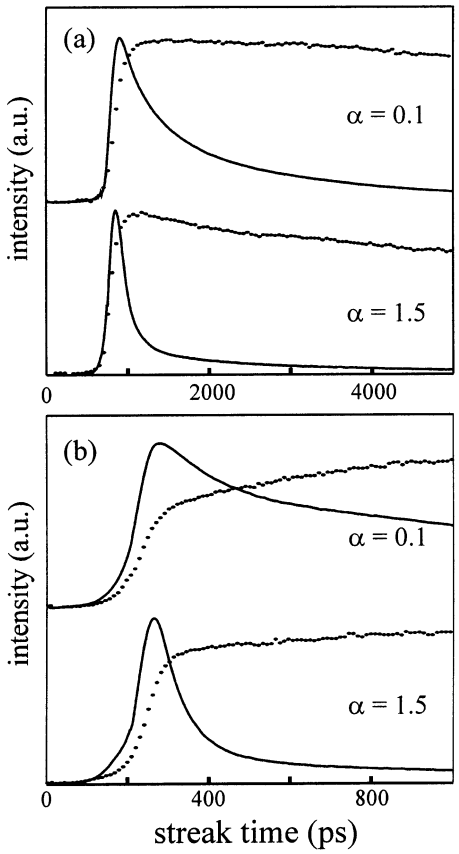

Figure 4. Fluorescence kinetic profiles of anthracene intercalated in NaY supercages with given α values, monitored at 400 ± 10 (solid) and 600 ± 10 nm (dotted) at long (a) and short (b) time windows.

600 nm to eliminate the interference of red-tailed monomeric fluorescence (Figure 4). The kinetics of monomeric fluorescence with $\alpha = 0.001$ can be adequately fitted with two exponential decays of 0.9 and 4 ns, indicating that anthracene monomers experience at least two different surroundings in the supercages of NaY. Anthracene molecules intercalated in the supercages of faujasite zeolites are often found to bind to very polar cationic sites or on supercage walls through electrostatic interactions.[38−41] A molecule is expected to have a shorter fluorescence lifetime at a cationic site than at a wall site because aromatic organic species are reported to have shorter fluorescence lifetimes in polar media than in nonpolar media and to relax rapidly via charge transfer at cationic sites.[25,38,42] Thus we ascribe 0.9 and 4 ns to the fluorescence-decay times of anthracene molecules adsorbed at cationic and wall sites, respectively.

Upon increasing the loading level of the guest molecules, quite interesting features of the fluorescence kinetics are

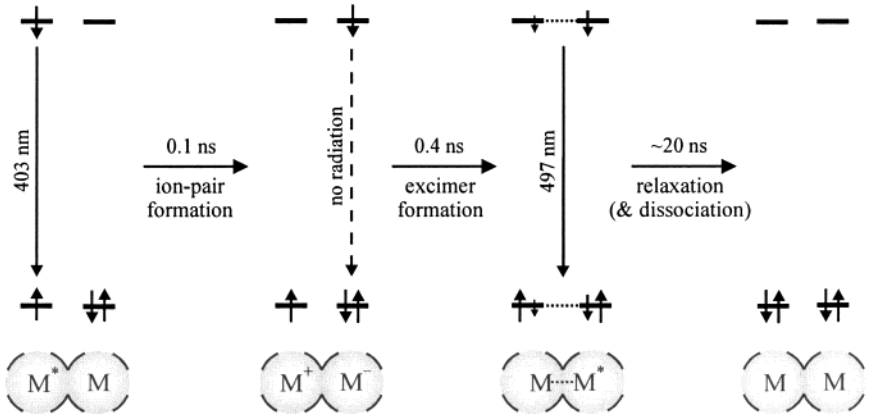

Figure 5. Proposed schematic orbital description for the photochemical-formation mechanism of an excimer from an excited anthracene molecule having another monomer in a nearest supercage. M denotes a monomer while M···M does a dimer.

TABLE 1: Fluorescence Kinetic Constants of Anthracene Adsorbed in the Supercages of NaY

	time (ns)	
α	decay at 400 nm[a]	rise at 600 nm[b]
0.001	0.9 (41%)[c] + 4 (59%)	
0.1	0.1 (45%) + 0.9 (43%) + 4 (12%)	fast (45%) + 0.4 (55%)
0.5	0.1 (67%) + 0.9 (27%) + 4 (6%)	fast (50%) + 0.4 (50%)
1.0	0.1 (79%) + 0.9 (17%) + 4 (4%)	fast (59%) + 0.4 (41%)
1.5	0.1 (91%) + 0.9 (7%) + 4 (2%)	fast (67%) + 0.4 (33%)

[a] Rises instantly. [b] Decays on the time scale of 20 ns. [c] Initial intensity percentage of each component.

recognized at both 400 and 600 nm: monomer fluorescence decays faster and excimer fluorescence rises slowly enough to resolve (Figure 4a). To look inside fast processes more precisely, we have investigated the fluorescence kinetics at a shorter time window (Figure 4b). Monomer fluorescence at high α values has an additional fast decay component of 0.1 ns (Table 1). The fractional amplitude of this component increases with the α increment at the expense of the amplitudes of the other two components. Thus we suggest that anthracene molecules giving the fast component of 0.1 ns bring in the formation of excimers. However, the time constants of all the three components do not change at all. This suggests that the three decay components of monomeric fluorescence arise from anthracene molecules having surroundings different nonequilibratorily within the relaxation time of excitation. The formation kinetics of excimeric fluorescence shows an instantly rising component with one rising on the time scale of 0.4 ns. It is intriguing that none of two excimeric-rise times is concurrent with the fast monomeric-decay time of 0.1 ns. The instant-rise component is ascribed to the excimer that is directly excited from the ground-state dimeric species, perceived already with the diffuse-reflectance spectra of Figure 2. On the other hand, the slow-rise component of 0.4 ns is attributed to excimers that are photochemically produced in the first-excited singlet state. The discrepancy between the fast decay time of monomer fluorescence and the slow rise time of excimer fluorescence implies that the photochemical formation of the excimeric species takes place in 0.4 ns following the formation of a nonluminescent intermediate transformed from the monomeric species in 0.1 ns.

Photochemical-Formation Mechanism of Excimers. The lack of intermediate fluorescence indicates that the intermediate species of photochemical excimer formation is nonradiative in our measured time domains. Then we can consider the intermediate to be the radical ion pair or the triplet-state monomer. We exclude the latter one because the excimer formed subsequently with a ground-state single monomer is fluorescent. We suggest that an excited monomer in a singly occupied supercage gives birth to an excimer if another monomer exists in a tetrahedrally connected nearest supercage (Figure 5). An excited monomer forms a nonluminescent ion pair with a monomer in a nearest supercage by transferring an electron within 0.1 ns.[25,39] The dark intermediate rearranges to transform into an excimer on the time scale of 0.4 ns. The radical ion pair is of course nonradiative because it is in the ground state. It is noteworthy that the formation time of the intermediate is about the same as the reported formation time of anthracene cations in NaX.[39,43] This designates that the formation rate of the ion pair is determined by the electron-ejection rate of the excited monomer. Strong Lewis-base sites in faujasite zeolites are negatively charged oxygen atoms to which cations are electrostatistically associated, whereas Lewis-acid sites are exchangeable cations. The concept of conjugate acid−base sites provides a picture that the formation of a radical ion pair by two anthracene molecules existing separately in two nearest supercages is triggered by ejection of an electron from an excited monomer. The ultrafast fluorescence quenching of probe molecules by quenchers located in adjacent supercages has been also explained by interactions of conjugate acid−base pairs.[43] Excimer formation (0.4 ns) is slower than ion-pair formation (0.1 ns), suggesting that the radical ion pair is required to undergo geometric rearrangement to obtain a proper orientation for the formation of the excimer. Two molecules located in two nearest supercages of NaY are reported to form a complex having a specific orientation.[44] Regardless of α variation, the invariable rate of photochemical excimer formation implies that inter-supercage diffusion of anthracene molecules does not take place to form excimers within the relaxation time of excited molecules at room temperature. The relaxation time of excimers (~20 ns) is much longer than those of excited monomers (0.9 and 4 ns), whereas the trend is opposite in solutions. Furthermore, excimer fluorescence is much stronger than monomer fluorescence at high loading levels, and the trend is also opposite in solutions. Thus, we consider that anthracene excimers formed in zeolitic nanocavities have good luminescence properties for optical applications.

Conclusions

Anthracene molecules can be optimally incorporated into catalytically important supercages of NaY at 570 K. Two anthracene molecules adsorb concertedly into a zeolitic supercage to form a ground-state stable dimer. The attractive forces are suggested to favor guest molecules energetically to form dimers during cooling after the diffusion process. An excited

monomer in a singly occupied supercage gives birth to an excimer if another monomer exists in a tetrahedrally connected nearest supercage. An excited monomer forms a nonluminescent ion pair with a monomer in a nearest supercage by transferring an electron within 0.1 ns. The dark intermediate rearranges to transform into an excimer on the time scale of 0.4 ns. Excimers relax in ~20 ns. On the other hand, isolated excited monomers show two decay times of 0.9 and 4 ns, depending on their adsorbed environment in zeolitic nanocavities.

Acknowledgment. We are greatly indebted to Professor Ryong Ryoo, Department of Chemistry, KAIST, Taejon 305-701, Korea, for helping us to measure NMR spectra. The Strategic National R&D Program is appreciated for Grant M1-0214-00-0108. D.J.J. and O.H.K. also thank the Center for Molecular Catalysis and the Brain Korea 21 Program, respectively.

References and Notes

(1) Chen, W.; Wang, Z. G.; Lin, Z. J.; Lin, L. Y. *Solid State Commun*. **1997**, *101*, 371.
(2) Gaare, K.; Akporiaye, D. *J. Phys. Chem. B* **1997**, *101*, 48.
(3) Takatani, S.; Fukumura, H.; Masuhara, H.; Hashimoto, S. *J. Phys. Chem. B* **1997**, *101*, 3365.
(4) Ryoo, R.; Cho, S. J.; Pak, C.; Lee, Y. J. *Catal. Lett*. **1993**, *20*, 107.
(5) Coleman, N. R. B.; Morris, M. A.; Spalding, T. R.; Holmes, J. D. *J. Am. Chem. Soc*. **2001**, *123*, 187.
(6) Han, Y.-J.; Kim, J. M.; Stucky, G. D. *Chem. Mater*. **2000**, *12*, 2068.
(7) Stucky, G. D.; MacDougall, J. E. *Science* **1990**, *247*, 669.
(8) Márquez, F.; Zicovich-Wilson, C. M.; Corma, A.; Palomares, E.; García, H. *J. Phys. Chem. B* **2001**, *105*, 9973.
(9) Márquez, F.; García, H.; Palomares, E.; Fernndez, L.; Corma, A. *J. Am. Chem. Soc*. **2000**, *122*, 6520.
(10) Joo, S. H.; Choi, S. J.; Oh, I.; Kwak, J.; Liu, Z.; Terasaki, O.; Ryoo, R. *Nature* **2001**, *412*, 169.
(11) Lee, J.-S.; Joo, S. H.; Ryoo, R *J. Am. Chem. Soc*. **2002**, *124*, 1156.
(12) Kwon, O.-H.; Yoo, H.; Park, K.; Tu, B.; Ryoo, R.; Jang, D.-J. *J. Phys. Chem. B* **2001**, *105*, 4195.
(13) Kwon, O.-H.; Park, K.; Jang, D.-J. *Chem. Phys. Lett*. **2001**, *346*, 195.
(14) Kwon, O.-H.; Yoo, H.; Jang, D.-J. *Eur. Phys. J. D* **2002**, *18*, 69.
(15) Cozens, F. L.; Régimbald, M.; García, H.; Scaiano, J. C. *J. Phys. Chem*. **1996**, *100*, 18165.
(16) Liu, X.; Iu, K.-K.; Thomas, J. K. *J. Phys. Chem*. **1994**, *98*, 7877.
(17) Yoon, K. B. *Chem. Rev*. **1993**, *93*, 321.
(18) Sykora, M.; Kincaid, J. R. *Nature* **1997**, *387*, 162.
(19) Hoppe, R.; Schulz-Ekloff, G.; Wöhrle, D.; Kirschhick, C.; Fuess, H. *Adv. Mater*. **1995**, *7*, 61.
(20) Pauchard, M.; Devaux, A.; Calzaferri, G. *Chem. Eur. J*. **2000**, *6*, 3456.
(21) Marlow, F.; McGehee, M. D.; Zhao, D.; Chmelka, B. F.; Stucky, G. D. *Adv. Mater*. **1999**, *11*, 632.
(22) Beddard, G. S.; Fleming, G. R.; Gijzeman, O. L. J.; Poter, G. *Proc. R. Soc. London, Ser. A* **1974**, *340*, 519.
(23) Ware, W. R.; Cunningham, P. T. *J. Chem. Phys*. **1965**, *45*, 11.
(24) Horiguchi, R.; Iwasaki, N.; Marutama, Y. *J. Phys. Chem*. **1987**, *91*, 5135.
(25) Hashimoto, S.; Fukazawa, N.; Fukumura, H.; Masuhara, H. *Chem. Phys. Lett*. **1994**, *219*, 445.
(26) Hashimoto, S.; Ikuta, S.; Asahi, T.; Masuhara, H. *Langmuir* **1998**, *14*, 4284.
(27) Iu, K.-K.; Thomas, J. K. *J. Phys. Chem*. **1991**, *95*, 506.
(28) Park, J.; Kang, W.-K.; Ryoo, R.; Jung, K.-H.; Jang, D.-J. *J. Photochem. Photobiol. A: Chem*. **1994**, *80*, 333.
(29) Chmelka, B. F.; Pearson, J. G.; Liu, S. B.; Ryoo, R.; de Menorval, L. C.; Pines, A. *J. Phys. Chem*. **1991**, *95*, 303.
(30) Sastre, G.; Cano, M. L.; Corma, A.; García, H.; Nicolopoulos, S.; González-Calbert, J. M.; Vallet-Regí, M. *J. Phys. Chem. B* **1997**, *101*, 10184.
(31) de Menorval, L. C.; Raftery, D.; Liu, S.-B.; Takegoshi, K.; Ryoo, R.; Pines, A. *J. Phys. Chem*. **1990**, *94*, 27.
(32) Ryoo, R.; Liu, S.-B.; de Menorval, L. C.; Takegoshi, K.; Chmelka, B.; Trecoske, M.; Pines, A. *J. Phys. Chem*. **1987**, *91*, 6575.
(33) Springuel-Huet, M.-A.; Bonardet, J.-L.; Gédéon, A.; Fraissard, J. *Magn. Reson. Chem*. **1999**, *37*, S1.
(34) Gédéon, A.; Bonardet, J. L.; Lepetit, C.; Fraissard, *J. Solid State NMR* **1995**, *5*, 201.
(35) Breck, D. W. *Zeolite Molecular Sieves: Structure, Chemistry, and Use*; John Wiley and Sons: New York, 1974.
(36) Uppili, S.; Thomas, K. J.; Crompton, E. M.; Ramamurthy, V. *Langmuir* **2000**, *16*, 265.
(37) Turro, N. J. *Modern Molecular Photochemistry*; University Science Book: Mill Valley, CA, 1991.
(38) Ramamurthy, V.; Sanderson, D. R.; Eaton, D. F. *J. Phys. Chem*. **1993**, *97*, 13380.
(39) Hashimoto, S.; Mutoh, T.; Fukumura, H.; Masuhara, H. *J. Chem. Soc., Faraday Trans*. **1996**, *92*, 3653.
(40) Hong, S. B.; Cho, H. M.; Davis, M. E. *J. Phys. Chem*. **1993**, *97*, 1622.
(41) Pearso, J. G.; Chmelka, B. F.; Shykind, D. N.; Pines, A. *J. Phys. Chem*. **1992**, *96*, 8517.
(42) Vasenkov, S.; Frei, H. *J. Am. Chem. Soc*. **1998**, *120*, 4031.
(43) Ellison, E. H.; Thomas, J. K. *Langmuir* **2001**, *17*, 2446.
(44) Kirschhock, C.; Fuess, H. *Microporous Mater*. **1997**, *8*, 19.